AGU100 ADVANCING EARTH AND SPACE SCIENCE

Geophysical Research Letters

RESEARCH LETTER

10.1029/2018GL078465

Shifts in Precipitation Accumulation Extremes During the Warm Season Over the United States

Cristian Martinez-Villalobos[1] and **J. David Neelin**[1]

[1]Department of Atmospheric and Oceanic Sciences, University of California, Los Angeles, Los Angeles, CA, U.S.A

Key Points:

- Probability densities of extreme accumulation events are controlled by a characteristic cutoff scale
- These cutoff scales exhibit increases for 1997–2013 versus 1979–1995 over substantial parts of the United States
- Associated changes in the distributions exemplify potential global warming distribution shifts

Supporting Information:

- Supporting Information S1

Correspondence to:
C. Martinez-Villalobos,
cmartinezvil@atmos.ucla.edu

Citation:
Martinez-Villalobos, C., & Neelin, J. D. (2018). Shifts in precipitation accumulation extremes during the warm season over the United States. *Geophysical Research Letters*, *45*, 8586–8595. https://doi.org/10.1029/2018GL078465

Received 21 APR 2018
Accepted 8 AUG 2018
Accepted article online 15 AUG 2018
Published online 30 AUG 2018

Abstract

Precipitation accumulations, integrated over precipitation events in hourly data, are examined from 1979 to 2013 over the contiguous United States during the *warm* season (May–October). As expected from theory, accumulation distributions have a characteristic shape, with an approximate power law decrease with event size followed by an exponential drop at a characteristic cutoff scale s_L for each location. This cutoff is a predictor of the highest accumulation percentiles and of a similarly defined daily precipitation cutoff P_L. Comparing 1997–2013 and 1979–1995 periods, there are significant regional increases in s_L in several regions. This yields distribution changes that are weighted disproportionately toward extreme accumulations. In the Northeast, for example, risk ratio (conditioned on occurrence) for accumulations larger than 109 mm increases by a factor of 2–4 (5th–95th). These changes in risk ratio as a function of size, and connection to underlying theory, have counterparts in the observed daily precipitation trends.

Plain Language Summary

Extreme accumulations of rainfall over a precipitation event can damage infrastructure, impact transportation, and be hazardous to human lives. For each region, there is a characteristic accumulation size that controls the probability of the most extreme accumulations. We show that this characteristic size has increased in several U.S. regions over recent decades. This implies an increase in the probability of extreme accumulations, which is expected to further intensify under future global warming.

1. Introduction

Increases in various extreme precipitation statistics have been documented over the United States during the twentieth century (Barbero et al., 2017; Easterling et al., 2017; Giorgi et al., 2011; Groisman et al., 2001, 2012; Karl & Knight, 1998; Karl et al., 2009; Kunkel et al., 1999; Kunkel, 2003; Melillo et al., 2014; Peterson et al., 2008), with increases projected to continue during the 21st century (Houghton et al., 2001; Janssen et al., 2016; Kunkel, Karl, Easterling, et al., 2013; Prein et al., 2017; Solomon et al., 2007; Stocker et al., 2013). During the warm season, changes in the 20-year return value of the daily precipitation totals over 1948–2015 generally show increases across most of the United States, with the largest increases during Fall (Easterling et al., 2017). Regionally, changes have been smaller in the western part of the country, and larger in the eastern part, especially in the Northeast (Balling & Goodrich, 2011; Huang et al., 2017). Leading order changes in extremes are understood to follow from increases in moisture associated to increases in temperature (Allen & Ingram, 2002; Fischer & Knutti, 2016; Pall et al., 2007; Singh & O'Gorman, 2014), which in the United States have steadily risen since the 1970s (Vose et al., 2017), especially during the warm season (Gleason et al., 2008). Up to this date, most studies have focused on changes in extremes in precipitation temporal averages, usually daily precipitation (Alexander et al., 2006; Easterling et al., 2017; Groisman et al., 2004; Pryor et al., 2009). In this study we expand upon the existing literature by focusing on changes in accumulation distributions.

Precipitation accumulations, the amount of precipitation integrated over the course of a storm event, is a variable of interest both physically and societally. Physically, in terms of the column water vapor budget, it represents the amount of water lost during the course of a storm event. Societal implications occur because extreme accumulation values are associated with flooding and associated hazards. Observations (DeLuca & Corral, 2014; Peters et al., 2001, 2010), theoretical modeling (Stechmann & Neelin, 2011, 2014, hereafter SN14; Neelin et al., 2017, hereafter NSSB17), and general circulation models (NSSB17) have established the general features of accumulation probability density functions (PDFs), which can be seen for a typical accumulation

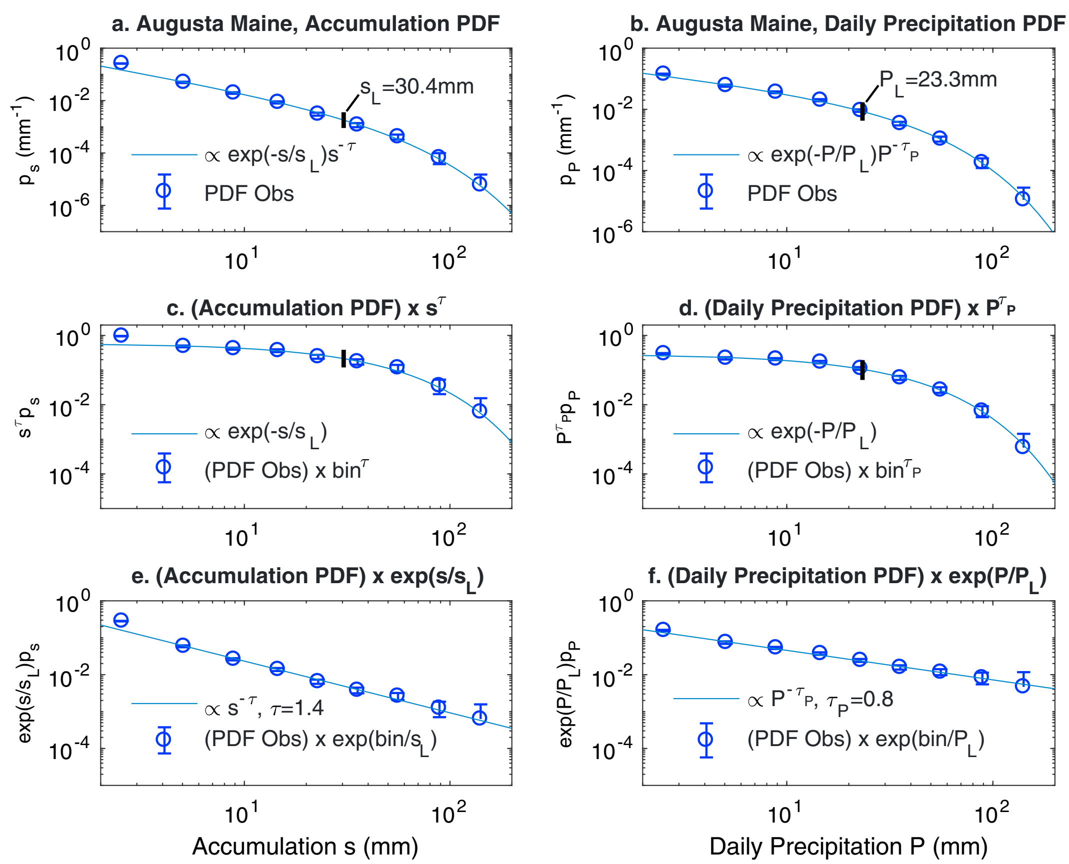

Figure 1. Augusta, Maine (a) accumulation and (b) daily precipitation PDFs. The circles represent the 50th and the error bars the 5th–95th percentiles based on 1,000 bootstrap (with replacement) realizations (Efron & Tibshirani, 1994). The solid lines represent fits given by equations (2) and (3) in the accumulation (a), and daily precipitation cases (b), respectively. The vertical line indicates the location of s_L or P_L. Panels (c) and (d) show tests for the *exponential* part of accumulation and daily precipitation distributions, and (e, f) for the *power law* part of accumulation and daily precipitation distributions.

distribution in Figure 1a (calculated using data from the Augusta (Maine) station, in the northeast part of the country). For accumulations larger than minimum instrumental resolution, small accumulations occur relatively more frequently, with probability slowly decaying approximately as a power law as event size increases, until encountering a characteristic cutoff scale s_L where probability drops much faster. Despite differences in location, the power law exponent (τ) appears to be relatively unaffected by local climate conditions (DeLuca & Corral, 2014; Peters et al., 2010), while the cutoff scale is a strong function of local climate (Peters et al., 2010). As is visually apparent in Figure 1c, the cutoff scale is important, as it controls the size of the largest accumulations at a given location.

Theory for accumulations (SN14; NSSB17) has established the dependence of the cutoff scale s_L on physical processes, specifically on the variability of moisture converging to/diverging from a precipitating column. Due to an increase in moisture availability, this cutoff scale is expected to increase under global warming (NSSB17). This is demonstrated in NSSB17, which compare present day with end of the 21st century accumulations using the Community Earth System Model. They found an almost exponential increase in the probability for the largest accumulations in many regions of the world, including several regions experiencing extreme events of size unprecedented in the current climate. This increase occurs in association to an increase in the cutoff scale for these regions.

An attractive feature of accumulation distributions is that they depend entirely on the precipitating regime dynamics—that is, the physical processes controlling wet spells—which does not hold true for daily precipitation, or other temporally averaged precipitation statistics, which inevitably include nonprecipitating regime effects. Given that there is theory connecting accumulation extremes to the size of moisture fluctuations, it is of interest to explore whether there is a relationship between accumulation and daily precipitation distribution parameters. For this reason, we repeat most of the analysis also for daily precipitation.

In this study we characterize the climatology and recent changes of accumulation distributions over the contiguous United States. We focus on changes in the cutoff scale instead of percentiles, because it is a physically motivated quantity whose estimators are more reliable and less sensitive to left-censored data than percentiles (see Text S1 in the supporting information). While emphasizing that it is not our intention to do an attribution of the changes, recent changes in probability distribution are evaluated for whether the form of the changes is consistent with a change in cutoff scale, as noted in model predictions for potential global warming effects. This paper is restricted to the U.S. warm season (May–October) to avoid issues related to measurement of liquid versus solid precipitation (Goodison et al., 1998; Groisman & Legates, 1994; Groisman et al., 1996; Rasmussen et al., 2012) in presence of changes in this partition (Déry & Brown, 2007; Kluver & Leathers, 2015; Kunkel et al., 2016; O'Gorman, 2014). Compared to other observational studies on accumulations (not necessarily based on the United States, Peters et al., 2001, 2010; DeLuca & Corral, 2014), this represents a considerable increase in both the temporal (on the order of decades) and spatial (covering the whole United States) scales involved.

2. Data and Methods

To calculate accumulations and daily precipitation, we use hourly precipitation data obtained from 1,276 stations (Figures 2a and 2b) that are part of the National Oceanic and Atmospheric Administration-National Centers for Environmental Information Climate Data Online system, covering the years 1979–2013 during May–October (the publicly available record ends in 2013). Details on the data set and criteria for data inclusion/exclusion are given in Text S2. The precipitation accumulation s, over the course of an event starting at time t_i and ending at t_f is given by

$$s = \int_{t_i}^{t_f} R(t)\mathrm{d}t, \tag{1}$$

where $R(t)$ is the precipitation intensity at time t. We calculate accumulations using a discretized version of the above equation. For each station consecutive nonzero hourly intensities are summed and constitute the accumulation s for a particular event. Daily (midnight to midnight) precipitation totals P are calculated from the same data set. When looking at changes in both accumulation and daily precipitation distributions, individual station time series are aggregated into seven different U.S. climate regions, as used in the Fourth National Climate Assessment (Wuebbles et al., 2017): Southwest, Northwest, Southern Plains, Northern Plains, Midwest, Southeast. and Northeast (Figure 3a). To test sensitivity against station proximity, we also carried a procedure where stations are aggregated in a 0.5° by 0.5° grid (Text S3), with similar results.

3. Accumulation and Daily Precipitation Distributions and Cutoff Scales

Previous observational studies (DeLuca & Corral, 2014; Peters et al., 2010) have established accumulations distributions (p_s) to be well approximated by

$$p_s \propto s^{-\tau} \exp(-s/s_L) \qquad s > s_{\min}, \tag{2}$$

with τ being the power law exponent, s_L an exponential cutoff scale, $s_{\min}$ a small accumulation value for which the aforementioned PDF form is valid. Similarly, daily precipitation PDFs (p_P) have often been fitted using Gamma distributions (Cho et al., 2004; Groisman et al., 1999; Ison et al., 1971; Katz, 1977; Richardson, 1981; Wilks, 1995):

$$p_P \propto P^{-\tau_P} \exp(-P/P_L), \qquad \tau_P < 1. \tag{3}$$

We note the similarity in the formulas for both distributions, with the main difference being in the power law exponents: for accumulations, typically $\tau > 1$, which indicates a steeper decay in the power law range. This is illustrated in Figures 1e and 1f where the difference in power law exponents is visually apparent. Note that the scale parameter P_L in the Gamma distribution can also be interpreted as a cutoff scale. Cutoff values s_L and P_L represent the size where the exponential part of the respective distributions decay to $1/e$ of their maxima (Figures 1b and 1d). Although the shapes of the distributions look similar, it is important to make an important

10.1029/2018GL078465

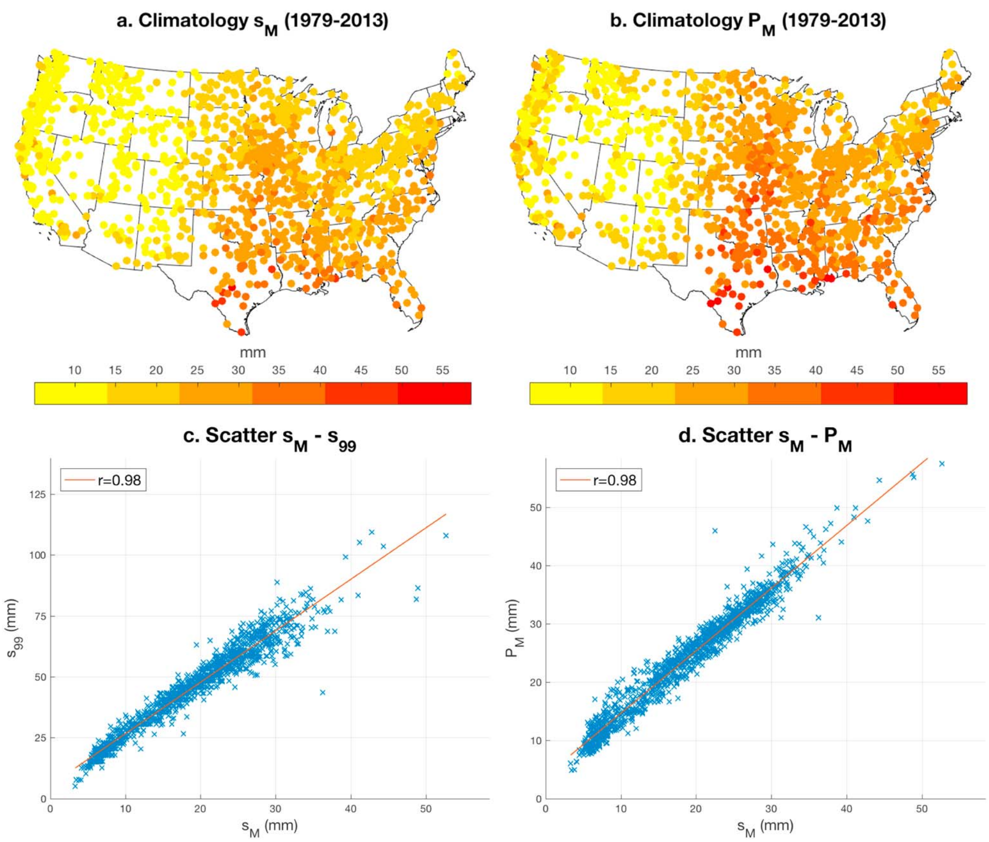

Figure 2. a (b) Individual stations s_M (P_M) climatology 1979–2013 (equation (4). (c) Scatter of s_M and accumulation 99th percentile s_{99} station values. (d) Scatter of s_M and P_M station values.

distinction between (2) and (3). The accumulation PDF basic shape (2) can be derived from first principles—by making use of the column moisture equation (SN14)—and as such it can be used to relate the accumulation PDFs with precipitation processes, whereas (3) is only an empirical fit.

For simplicity, we use moment ratios s_M and P_M as estimators of the cutoffs s_L (Peters et al., 2010; SN14; see also Muschinski and Katz, 2013) and P_L for most of the rest of the paper. These moments ratio are defined as

$$s_M = \frac{< s^2 >}{< s >}, P_M = \frac{< P^2 >}{< P >}. \tag{4}$$

This choice has the advantage of being independent on fitting assumptions. Note that both accumulation (2) and daily precipitation (3) PDFs are calculated only for nonzero totals. An approximately logarithmic scheme, which closely follows Quinn and Neelin (2017), is used to calculate PDFs.

4. Results

4.1. Accumulation and Daily Precipitation Cutoff Scales Climatology

Figure 2a shows the s_M climatology over the United States for the 1979–2013 period. We observe that s_M is a strong function of local climate, with geographical variations conforming to expectations—that is, larger values over wetter regions and smaller values over dryer regions for this season. We note relatively large values for the coastal Pacific regions, associated mainly with precipitation in late Spring/early Fall. The cutoff scale s_L, or its proxy s_M, is related to the highest accumulation percentiles. This can be seen in Figure 2c, which shows the scatter of s_M with the accumulation 99th percentile s_{99} at each station ($r = 0.98$). Similar relations exist with the 95th and 99.9th percentiles. The spatial variability of P_M (Figure 2b) shows an important degree of correspondence to s_M spatial variability. The scatter of the s_M and P_M station values (Figure 2d) confirms this relation ($r = 0.98$).

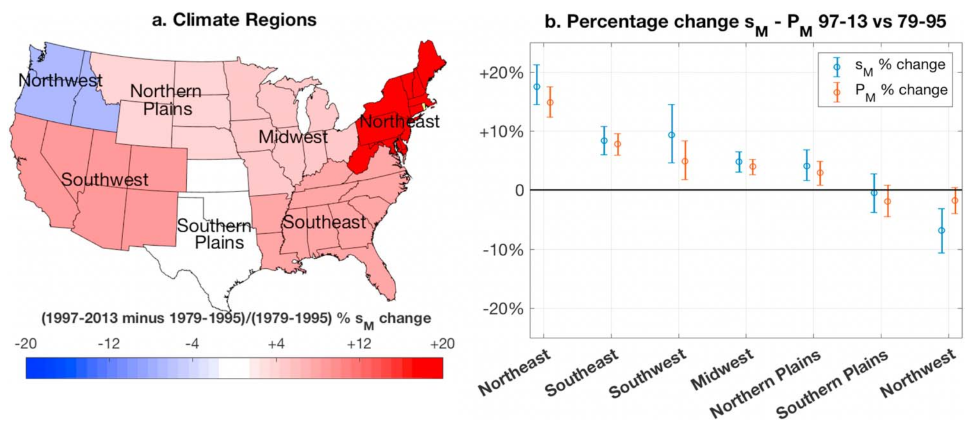

Figure 3. (a) Climate regions used in this study. These regions are the same as defined in Wuebbles et al. (2017). Each region is color coded by the median s_M percentage change between 1979–1995 and 1997–2013. (b) Accumulation and daily precipitation moments ratios (s_M and P_M) percentage change between 1979–1995 and 1997–2013 for the regions defined in (a). The circles represent the 50th and the error bars the 5th-95th percentiles based on 1,000 bootstrap (with replacement) realizations.

4.2. Increases in Cutoff Scales Comparing 1997–2013 With 1979–1995

Figure 3b shows the percentage change in s_M and P_M when comparing the 1997–2013 period to the baseline 1979–1995 period. Significant increases are found in the Northeast, Southeast, Southwest, Midwest, Northern Plains, no significant change is found in the Southern Plains, and actually a significant decrease in s_M is found in the Northwest. Changes in daily precipitation and accumulation cutoff scales are consistent between each other, but with changes in P_M being generally smaller in amplitude. Of note is the behavior of s_M and P_M changes in the Southwest where the increase in P_M ($\sim +5\%$) is much smaller than the increase in s_M ($\sim +10\%$), and in the Northwest where s_M has had a significant decrease of $\sim -7\%$, whereas P_M has not changed significantly between these two periods. We note that results for P_M are largely consistent with previously reported trends (Easterling et al., 2017; Groisman et al., 2001; Karl & Knight, 1998; Kunkel, 2003; Peterson

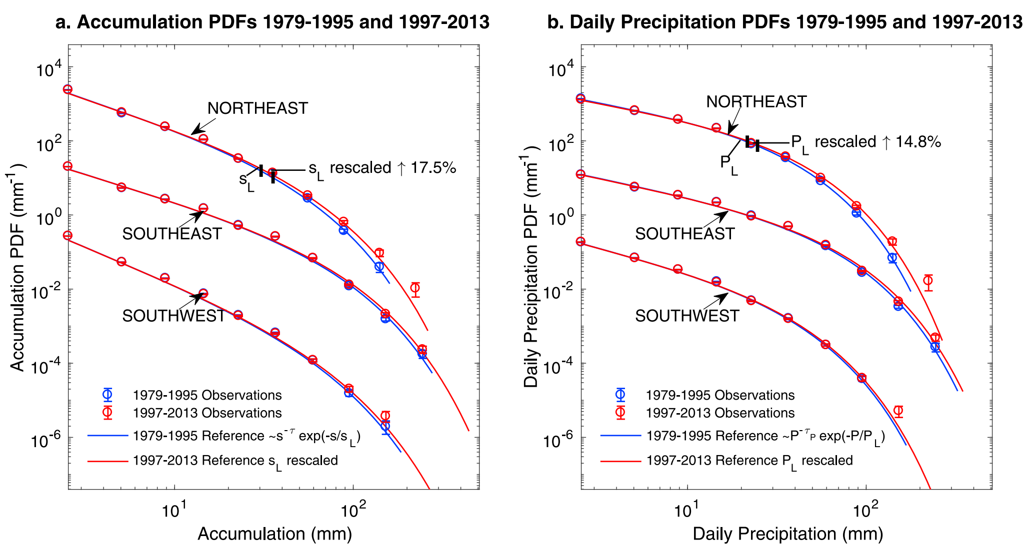

Figure 4. Accumulation (a) and daily precipitation (b) PDFs calculated over the 1979–1995 (blue) and 1997–2013 (red) periods for the three regions with biggest s_M increases in Figure 3b ($\times 10^4$ Northeast and $\times 10^2$ Southeast PDFs). Only bins with 10 or more counts are displayed. The circles represent the 50th and the error bars the 5th–95th percentiles based on 1,000 bootstrap (with replacement) realizations. A reference line $As^{-\tau}\exp(-s/s_L)$ (or $BP^{-\tau_P}\exp(-P/P_L)$) is superimposed over 1979–1995 accumulations (daily precipitation) observed PDF, and a rescaled version of it with increased s_L (P_L) is superimposed over the 1997–2013 observed PDFs. The rescaled values are given by the median s_M or P_M increases over these regions (Figure 3b). The reference lines run up to the largest accumulation or daily precipitation in each period. See Figure S7 in the supporting information for a version with a linear y axis.

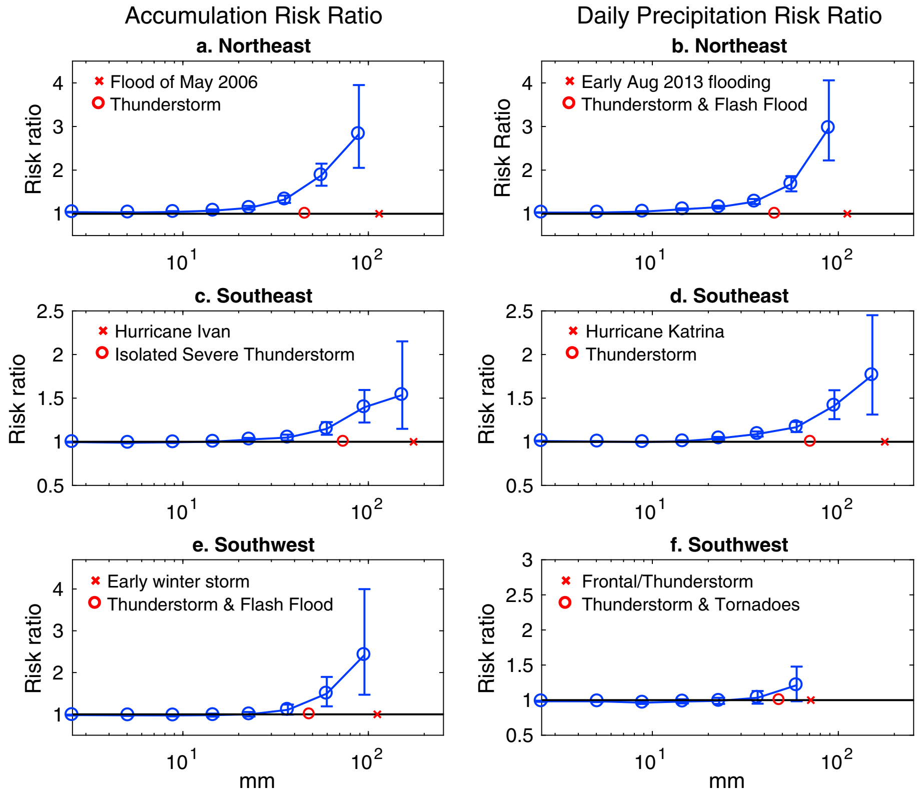

Figure 5. Accumulation (a, c, and e) and daily precipitation (b, d, and f) conditional risk ratios (5) for the three regions with largest s_M increases (Figure 3). Note that due to the risk ratio being an integrated quantity, the number of bins displayed is one less compared to Figure 4 1979–1995 distributions (which contains fewer extreme events). Confidence intervals are assessed from 1,000 bootstrap realizations, as in the previous figures. Each panel shows an example of a high-impact meteorological event (*x*), as well as a moderately impactful but more frequent event (*o*) for context (see Text S6 for more details). Note that because the dataset covers only up to 2013, recent high-impact events (e.g., van der Wiel et al., 2017; van Oldenborgh et al., 2017) are not included.

et al., 2008) in other daily extreme precipitation statistics during the last decades, that is, a larger fraction of extreme events in recent periods (with differences discussed in Text S4). Because accumulations result purely from the precipitating regime, they can naturally be broken into effects of event duration and mean intensity. Although extreme hourly intensities exhibit modest increases, these are not associated with changes in the largest accumulations. Rather, regions exhibiting substantial changes in probability of large accumulations are explained primarily by changes in the average *duration* of those events (cf. Dwyer & O'Gorman 2017; see Text S5 for details).

To examine the shape of the change in the PDF associated with changes in moment ratio, we plot the accumulation and daily precipitation distributions in both periods for the three regions with the largest increases (Figure 3) in Figure 4. We note that we do not have enough data to properly represent the largest few events (bins with <10 counts) in some regions, so to give a sense of the associated probabilities, we include a fit that runs up to the largest event in each period (Text S6 and Table S1). Comparing both periods, relative changes in both accumulation and daily precipitation distributions are larger in the tails. That is, there is a larger fraction of extreme events in the latter period compared to the former. These increases in extreme accumulations fraction are associated with an increase in cutoff scale s_L in agreement with theory (NSSB17). Rescaling the 1979–1995 distributions by the median increase in s_M (Figure 3b) provides a good representation of the distributions in the latter period, although it tends to underestimate the increases in the largest events. Figure 4b shows that a similar rescaling of the distribution (Pendergrass & Hartmann, 2014) occurs for daily precipitation.

While keeping in mind that decadal variability effects (Deser et al., 2012; Hoerling et al., 2016; Huang et al., 2018) may be present in these results for 17-year intervals, the changes in the shape of the probability distribution for the largest accumulations are in line with changes in the cutoff scale noted for simulations of future changes in the distribution (NSSB17) and may potentially have dramatic impacts on the associated large event risks (Otto et al., 2012; NSSB17) if trends were to continue. One way to illustrate this is by the calculation of conditional (conditioned on event occurrence) risk ratios, defined as

$$r_s(\hat{s}) = \frac{\int_{\hat{s}}^{\infty} p_{s'}^{II} \mathrm{d}s'}{\int_{\hat{s}}^{\infty} p_{s'}^{I} \mathrm{d}s'}. \tag{5}$$

This corresponds to the ratio of the probability of accumulations larger than $\hat{s}$ between periods II (1997–2013) and I (1979–1995). For accumulations, conditional risk ratios depend solely on changes in the precipitating regime dynamics, and thus they give information about changes related to precipitating processes. Accumulations, and similarly defined daily precipitation risk ratios are shown in Figure 5 for the same three regions shown in Figure 4. For small accumulations this ratio is close to 1, but increases roughly exponentially as accumulation size increases for these regions (see also NSSB17, Figure 2). For example, the risk ratio for accumulations larger than the upper bin (upper bin edge 109 mm) shows an increase by a factor of 2–4 (5th–95th) in the latter period compared to the former in the Northeast. Smaller, but significant increases occur for the Southeast, Southwest, Northern Plains, and Midwest regions (Figure S8). Similar risk ratios are calculated for daily precipitation (see also Figure S9). We note that the form of this accumulation, or daily precipitation, risk ratio is consistent with an increase in the cutoff scale for distributions of the form (2) and (3).

The number of events depends strongly on the dynamics governing dry spells (Lau et al., 2013; Rajah et al., 2014, SN14). In several of the regions here, the number of events decrease in period II relative to I, for example, by approximately 13% in the Northeast (only taking into account stations with full record). A contributing factor to this may be the decrease of summertime extra tropical activity in North America since 1979 (Chang et al., 2016). Despite the decrease in the total number of events, the number of extreme events increase in most regions, with an increase of ~80% of accumulations larger than 68 mm in 1997–2013 compared to 1979–1995 in the Northeast. We note the daily averages typically span both precipitating and nonprecipitating times, and thus tend to combine these opposing tendencies. The precipitating regime apparently dominates the observed changes, such that the change in the daily distribution tends to follow that of the accumulation distribution although with a less clear signal (Figure 3b, also compare Figures S8 and S9).

5. Summary and Discussion

Precipitation accumulation distributions from hourly precipitation data for the U.S. warm season are found to conform to the theoretically expected shape, with a power law range followed by an exponential cutoff for large accumulations. This cutoff s_L marks the typical accumulation size where the probability of occurrence drops sharply, hence limiting the probability of the most extreme events. Accumulation cutoff scales are strong functions of local climate, with larger values in generally wetter regions during this season. We show this cutoff scale to be related to the highest accumulation percentiles, as well as being a predictor to a similarly defined daily precipitation cutoff scale. The relationship between cutoff scales is relevant,because it allows theory for changes in accumulation distributions under global warming (with s_L scaling with moisture, see NSSB17) to be approximately translated to daily averaged intensities as well.

Comparing 1979–1995 and 1997–2013, spatially aggregated data show increases in both daily precipitation and accumulation cutoff scales in most regions, with the biggest increases occurring in the Northeast. Changes in daily precipitation cutoff scale follow changes in accumulation cutoff, although they are somewhat smaller in magnitude. Associated changes in the accumulation and daily precipitation distributions show that small event probabilities do not change significantly between periods and that increases in cutoff scales are associated with an increase in the probability of extremes, in agreement with Kunkel, Karl, Brooks, et al. (2013). This increase results in large, roughly exponential, increases in conditional risk ratio, for both accumulations and daily precipitation, as size increase in five out of seven regions, especially in the eastern part of the country. For example, a conditional risk ratio increase of a factor of 3 is found in the Northeast for accumulations larger than 109 mm. We note that the relation between s_L and P_L justifies the use of empirical statistical models based on the scale parameter (our P_L) of Gamma distributions to explain disproportionate increases in heavy precipitation (e.g., Groisman et al., 1999; Wilby & Wigley, 2002).

Theory for accumulations predicts changes of the *distribution*, specifically s_L scaling with column water vapor increases. While underlining the caveat that this is not an attribution study, the conditional risk ratio increases shown in Figure 5 have a form consistent with those projected under global warming (NSSB17). The conditional risk ratio increases of high-impact meteorological events (Figure 5), as well as of less impactful but more frequent events such as summer thunderstorm systems (Figure 5) thus typify changes that may be anticipated (Allen & Ingram, 2002; NSSB17; O'Gorman, 2015; Pfahl et al., 2017; Schneider et al., 2010; Tebaldi et al., 2006; Trenberth et al., 2003) as moisture availability increases in a warming world.

Societal infrastructure is adapted to local historical precipitation and accumulation distributions. As suggested by the rescaling in Figure 4, both accumulation and daily precipitation cutoff scales (or moment ratios) are useful quantities that provide information on leading order changes in the associated distributions; hence, they may provide practical guidance for adaptation efforts. Here we see increases in large accumulations, even while the total number of events decreases, consistent with more extensive dry spells (e.g., Giorgi et al., 2011). The daily averaged intensities tend to combine opposing effects from the precipitating and nonprecipitating regimes. The changes in the distribution of accumulations are thus useful in providing a measure of the changes occurring purely in the precipitating regime.

Acknowledgments
This research was supported by National Science Foundation grant AGS-1540518 and National Oceanic and Atmospheric Administration grants NA15OAR4310097 and NA14OAR4310274. U.S. hourly precipitation data are courtesy of the NOAA-NCEI Climate Data Online system https://www.ncdc.noaa.gov/cdo-web/search?datasetid=PRECIP_HLY\#. CPC US Unified Precipitation Data (Chen et al., 2008; Xie et al., 2007) provided by the NOAA/OAR?ESRL PSD, Boulder, Colorado, USA. We thank J. Meyerson for data management assistance. A portion of this work has previously been presented at an American Geophysical Union meeting (Martinez-Villalobos & Neelin, 2017).

References

Alexander, L. V., Zhang, X., Peterson, T. C., Caesar, J., Gleason, B., Klein Tank, A. M. G., et al. (2006). Global observed changes in daily climate extremes of temperature and precipitation. *Journal of Geophysical Research*, *111*, D05109. https://doi.org/10.1029/2005JD006290

Allen, M. R., & Ingram, W. J. (2002). Constraints on future changes in climate and the hydrologic cycle. *Nature*, *419*(6903), 224–232. https://doi.org/10.1038/nature01092

Balling, R. C., & Goodrich, G. B. (2011). Spatial analysis of variations in precipitation intensity in the USA. *Theoretical and Applied Climatology*, *104*(3-4), 415–421. https://doi.org/10.1007/s00704-010-0353-0

Barbero, R., Fowler, H. J., Lenderink, G., & Blenkinsop, S. (2017). Is the intensification of precipitation extremes with global warming better detected at hourly than daily resolutions? *Geophysical Research Letters*, *44*, 974–983. https://doi.org/10.1002/2016GL071917

Chang, E. K. M., Ma, C.-G., Zheng, C., & Yau, A. M. W. (2016). Observed and projected decrease in Northern Hemisphere extratropical cyclone activity in summer and its impacts on maximum temperature. *Geophysical Research Letters*, *43*, 2200–2208. https://doi.org/10.1002/2016GL068172

Chen, M., Shi, W., Xie, P., Silva, V. B. S., Kousky, V. E., Wayne Higgins, R., & Janowiak, J. E. (2008). Assessing objective techniques for gauge-based analyses of global daily precipitation. *Journal of Geophysical Research*, *113*, D04110. https://doi.org/10.1029/2007JD009132

Cho, H.-K., Bowman, K. P., & North, G. R. (2004). A comparison of gamma and lognormal distributions for characterizing satellite rain rates from the tropical rainfall measuring mission. *Journal of Applied Meteorology*, *43*, 1586–1597.

DeLuca, A., & Corral, Á. (2014). Scale invariant events and dry spells for medium-resolution local rain data. *Nonlinear Processes in Geophysics*, *21*, 555–567. https://doi.org/10.5194/npg-21-555-2014

Déry, S. J., & Brown, R. D. (2007). Recent Northern Hemisphere snow cover extent trends and implications for the snow-albedo feedback. *Geophysical Research Letters*, *34*, L22504. https://doi.org/10.1029/2007GL031474

Deser, C., Phillips, A., Bourdette, V., & Teng, H. (2012). Uncertainty in climate change projections: The role of internal variability. *Climate Dynamics*, *38*(3-4), 527–546. https://doi.org/10.1007/s00382-010-0977-x

Dwyer, J. G., & O'Gorman, P. A. (2017). Changing duration and spatial extent of midlatitude precipitation extremes across different climates. *Geophysical Research Letters*, *44*, 5863–5871. https://doi.org/10.1002/2017GL072855

Easterling, D., Kunkel, K., Arnold, J., Knutson, T., LeGrande, A., Leung, L., et al. (2017). Precipitation change in the United States. In D. J. Wuebbles, et al. (Eds.), *Climate Science Special Report: Fourth National Climate Assessment* (Vol. 1, pp. 207–230). https://doi.org/10.7930/J0H993CC

Efron, B., & Tibshirani, R. (1994). *An Introduction to the Bootstrap* (436 pp.). London, New York: Chapman & Hall.

Fischer, E. M., & Knutti, R. (2016). Observed heavy precipitation increase confirms theory and early models. *Nature Climate Change*, *6*(11), 986–991. https://doi.org/10.1038/nclimate3110

Giorgi, F., Im, E.-S., Coppola, E., Diffenbaugh, N. S., Gao, X. J., Mariotti, L., & Shi, Y. (2011). Higher hydroclimatic intensity with global warming. *Journal of Climate*, *24*(20), 5309–5324. https://doi.org/10.1175/2011JCLI3979.1

Gleason, K. L., Lawrimore, J. H., Levinson, D. H., Karl, T. R., & Karoly, D. J. (2008). A revised U.S. climate extremes index. *Journal of Climate*, *21*(10), 2124–2137. https://doi.org/10.1175/2007JCLI1883.1

Goodison, B., Louie, P., & Yang, D. (1998). WMO solid precipitation measurement intercomparison. Instruments and observing methods. Report No. 67. WMO/TD - No. 872 (Tech. Rep.). Geneva, Switzerland: World Meteorological Organization.

Groisman, P. Y., Easterling, D. R., Quayle, R. G., Golubev, V. S., Krenke, A. N., & Mikhailov, A. Y. (1996). Reducing biases in estimates of precipitation over the United States: Phase 3 adjustments. *Journal of Geophysical Research*, *101*(D3), 7185–7195. https://doi.org/10.1029/95JD02600

Groisman, P. Y., Karl, T. R., Easterling, D. R., Knight, R. W., Jamason, P. F., Hennessy, K. J., et al. (1999). Changes in the probability of heavy precipitation: Important indicators of climatic change. *Climatic Change*, *42*(1), 243–283. https://doi.org/10.1023/A:1005432803188

Groisman, P. Y., Knight, R. W., & Karl, T. R. (2001). Heavy precipitation and high streamflow in the contiguous United States: Trends in the twentieth century. *Bulletin of the American Meteorological Society*, *82*(2), 219–246. https://doi.org/10.1175/1520-0477(2001)082<0219:HPAHSI>2.3.CO;2

Groisman, P. Y., Knight, R. W., & Karl, T. R. (2012). Changes in intense precipitation over the Central United States. *Journal of Hydrometeorology*, *13*(1), 47–66. https://doi.org/10.1175/JHM-D-11-039.1

Groisman, P. Y., Knight, R. W., Karl, T. R., Easterling, D. R., Sun, B., & Lawrimore, J. H. (2004). Contemporary changes of the hydrological cycle over the contiguous United States: Trends derived from in situ observations. *Journal of Hydrometeorology*, *5*(1), 64–85. https://doi.org/10.1175/1525-7541(2004)005<0064:CCOTHC>2.0.CO;2

Groisman, P. Y., & Legates, D. R. (1994). The accuracy of United States precipitation data. *Bulletin of the American Meteorological Society*, *75*(2), 215–227. https://doi.org/10.1175/1520-0477(1994)075<0215:TAOUSP>2.0.CO;2

Hoerling, M., Eischeid, J., Perlwitz, J., Quan, X.-W., Wolter, K., & Cheng, L. (2016). Characterizing recent trends in U.S. heavy precipitation. *Journal of Climate*, *29*(7), 2313–2332. https://doi.org/10.1175/JCLI-D-15-0441.1

Houghton, J. T., Ding, Y., Griggs, D. J., Noguer, M., van der Linden, P. J., Dai, X., et al. (2001). Climate change 2001: The scientific basis. Contribution of Working Group I to the Third Assessment Report of the Intergovernmental Panel on Climate Change, *Climate Change 2001: The Scientific Basis. Contribution of Working Group I to the Third Assessment Report of the Intergovernmental Panel on Climate Change* (Vol. 22, pp. 1144–1144). Cambridge, UK: Cambridge University Press. https://doi.org/10.1256/004316502320517344

Huang, H., Winter, J. M., & Osterberg, E. C. (2018). Mechanisms of abrupt extreme precipitation change over the Northeastern United States. *Journal of Geophysical Research: Atmospheres*, *123*. https://doi.org/10.1029/2017JD028136

Huang, H., Winter, J. M., Osterberg, E. C., Horton, R. M., & Beckage, B. (2017). Total and extreme precipitation changes over the Northeastern United States. *Journal of Hydrometeorology*, *18*(6), 1783–1798. https://doi.org/10.1175/JHM-D-16-0195.1

Ison, N. T., Feyerherm, A. M., & Bark, L. D. (1971). Wet period precipitation and the gamma distribution. *Journal of Applied Meteorology*, *10*(4), 658–665. https://doi.org/10.1175/1520-0450(1971)010<0658:WPPATG>2.0.CO;2

Janssen, E., Sriver, R. L., Wuebbles, D. J., & Kunkel, K. E. (2016). Seasonal and regional variations in extreme precipitation event frequency using CMIP5. *Geophysical Research Letters*, *43*, 5385–5393. https://doi.org/10.1002/2016GL069151

Karl, T. R., & Knight, R. W. (1998). Secular trends of precipitation amount, frequency, and intensity in the United States. *Bulletin of the American Meteorological Society*, *79*(2), 231–241. https://doi.org/10.1175/1520-0477(1998)079<0231:STOPAF>2.0.CO;2

Karl, T. R., Melillo, J. M., & Peterson, T. C. (2009). *Global Climate Change Impacts in the United States*. Cambridge, New York: Cambridge University Press.

Katz, R. W. (1977). Precipitation as a chain-dependent process. *Journal of Applied Meteorology*, *16*(7), 671–676. https://doi.org/10.1175/1520-0450(1977)016<0671:PAACDP>2.0.CO;2

Kluver, D., & Leathers, D. (2015). Regionalization of snowfall frequency and trends over the contiguous United States. *International Journal of Climatology*, *35*(14), 4348–4358. https://doi.org/10.1002/joc.4292

Kunkel, K. E. (2003). North American trends in extreme precipitation. *Natural Hazards*, *29*(2), 291–305. https://doi.org/10.1023/A:1023694115864

Kunkel, K. E., Andsager, K., & Easterling, D. R. (1999). Long-term trends in extreme precipitation events over the conterminous United States and Canada. *Journal of Climate*, *12*(8), 2515–2527. https://doi.org/10.1175/1520-0442(1999)012<2515:LTTIEP>2.0.CO;2

Kunkel, K. E., Karl, T. R., Brooks, H., Kossin, J., Lawrimore, J. H., Arndt, D., et al. (2013). Monitoring and understanding trends in extreme storms: State of knowledge. *Bulletin of the American Meteorological Society*, *94*(4), 499–514. https://doi.org/10.1175/BAMS-D-11-00262.1

Kunkel, K. E., Karl, T. R., Easterling, D. R., Redmond, K., Young, J., Yin, X., & Hennon, P. (2013). Probable maximum precipitation and climate change. *Geophysical Research Letters*, *40*, 1402–1408. https://doi.org/10.1002/grl.50334

Kunkel, K. E., Robinson, D. A., Champion, S., Yin, X., Estilow, T., & Frankson, R. M. (2016). Trends and extremes in Northern Hemisphere snow characteristics. *Current Climate Change Reports*, *2*(2), 65–73. https://doi.org/10.1007/s40641-016-0036-8

Lau, W. K.-M., Wu, H.-T., & Kim, K.-M. (2013). A canonical response of precipitation characteristics to global warming from CMIP5 models. *Geophysical Research Letters*, *40*, 3163–3169. https://doi.org/10.1002/grl.50420

Martinez-Villalobos, C., & Neelin, J. D. (2017). Shifts in summertime precipitation accumulation distributions over the US. In *American Geophysical Union, Fall Meeting 2017*. Abstract A41K-06.

Melillo, J. M., Richmond, T. C., Yohe, G. W., & Office, U. S. G. P. (2014). Climate change impacts in the United States: The third national climate assessment (Tech. Rep.). Washington, DC: U.S. Global Change Research Program. https://doi.org/10.7930/J0Z31WJ2

Muschinski, T., & Katz, J. I. (2013). Trends in hourly rainfall statistics in the United States under a warming climate. *Nature Climate Change*, *3*(6), 577–580. https://doi.org/10.1038/nclimate1828

Neelin, J. D., Sahany, S., Stechmann, S. N., & Bernstein, D. N. (2017). Global warming precipitation accumulation increases above the current-climate cutoff scale. *Proceedings of the National Academy of Sciences of the United States of America*, *114*(6), 1258–1263. https://doi.org/10.1073/pnas.1615333114

O'Gorman, P. A. (2014). Contrasting responses of mean and extreme snowfall to climate change. *Nature*, *512*(7515), 416–418. https://doi.org/10.1038/nature13625

O'Gorman, P. A. (2015). Precipitation extremes under climate change. *Current Climate Change Reports*, *1*(2), 49–59. https://doi.org/10.1007/s40641-015-0009-3

Otto, F. E. L., Massey, N., van Oldenborgh, G. J., Jones, R. G., & Allen, M. R. (2012). Reconciling two approaches to attribution of the 2010 Russian heat wave. *Geophysical Research Letters*, *39*, L04702. https://doi.org/10.1029/2011GL050422

Pall, P., Allen, M. R., & Stone, D. A. (2007). Testing the Clausius–Clapeyron constraint on changes in extreme precipitation under CO_2 warming. *Climate Dynamics*, *28*(4), 351–363. https://doi.org/10.1007/s00382-006-0180-2

Pendergrass, A. G., & Hartmann, D. L. (2014). Two modes of change of the distribution of rain*. *Journal of Climate*, *27*(22), 8357–8371. https://doi.org/10.1175/JCLI-D-14-00182.1

Peters, O., Deluca, A., Corral, A., Neelin, J. D., & Holloway, C. E. (2010). Universality of rain event size distributions. *Journal of Statistical Mechanics: Theory and Experiment*, *2010*(11), P11030. https://doi.org/10.1088/1742-5468/2010/11/P11030

Peters, O., Hertlein, C., & Christensen, K. (2001). A complexity view of rainfall. *Physical Review Letters*, *88*(1), 018701. https://doi.org/10.1103/PhysRevLett.88.018701

Peterson, T. C., Zhang, X., Brunet-India, M., & Vázquez-Aguirre, J. L. (2008). Changes in North American extremes derived from daily weather data. *Journal of Geophysical Research*, *113*, D07113. https://doi.org/10.1029/2007JD009453

Pfahl, S., O'Gorman, P. A., & Fischer, E. M. (2017). Understanding the regional pattern of projected future changes in extreme precipitation. *Nature Climate Change*, *7*, 423–427.

Prein, A. F., Rasmussen, R. M., Ikeda, K., Liu, C., Clark, M. P., & Holland, G. J. (2017). The future intensification of hourly precipitation extremes. *Nature Climate Change*, *7*(1), 48–52. https://doi.org/10.1038/nclimate3168

Pryor, S. C., Howe, J. A., & Kunkel, K. E. (2009). How spatially coherent and statistically robust are temporal changes in extreme precipitation in the contiguous USA? *International Journal of Climatology*, *29*(1), 31–45. https://doi.org/10.1002/joc.1696

Quinn, K. M., & Neelin, J. D. (2017). Distributions of tropical precipitation cluster power and their changes under global warming. Part I: Observational baseline and comparison to a high-resolution atmospheric model. *Journal of Climate*, *30*(20), 8033–8044. https://doi.org/10.1175/JCLI-D-16-0683.1

Rajah, K., O'Leary, T., Turner, A., Petrakis, G., Leonard, M., & Westra, S. (2014). Changes to the temporal distribution of daily precipitation. *Geophysical Research Letters*, *41*, 8887–8894. https://doi.org/10.1002/2014GL062156

Rasmussen, R., Baker, B., Kochendorfer, J., Meyers, T., Landolt, S., Fischer, A. P., et al. (2012). How well are we measuring snow: The NOAA/FAA/NCAR winter precipitation test bed. *Bulletin of the American Meteorological Society*, *93*(6), 811–829. https://doi.org/10.1175/BAMS-D-11-00052.1

Richardson, C. W. (1981). Stochastic simulation of daily precipitation, temperature, and solar radiation. *Water Resources Research*, *17*, 182–190. https://doi.org/10.1029/WR017i001p00182

Schneider, T., O'Gorman, P. A., & Levine, X. J. (2010). Water vapor and the dynamics of climate changes. *Reviews of Geophysics*, *48*, RG3001. https://doi.org/10.1029/2009RG000302

Singh, M. S., & O'Gorman, P. A. (2014). Influence of microphysics on the scaling of precipitation extremes with temperature. *Geophysical Research Letters*, *41*, 6037–6044. https://doi.org/10.1002/2014GL061222

Solomon, S., Qin, D., Manning, M., Chen, Z., Marquis, M., Averyt, K., et al. (Eds.) (2007). *Climate change 2007 - The physical science basis*, *Working Group I Contribution to the Fourth Assessment Report of the IPCC* (pp. 996). Cambridge, UK: Cambridge University Press. https://doi.org/10.1260/095830507781076194

Stechmann, S. N., & Neelin, J. D. (2011). A stochastic model for the transition to strong convection. *Journal of the Atmospheric Sciences*, *68*(12), 2955–2970. https://doi.org/10.1175/JAS-D-11-028.1

Stechmann, S. N., & Neelin, J. D. (2014). First-passage-time prototypes for precipitation statistics. *Journal of the Atmospheric Sciences*, *71*(9), 3269–3291. https://doi.org/10.1175/JAS-D-13-0268.1

Stocker, T., Qin, D., Plattner, G.-K., Tignor, M., Allen, S., Boschung, J., et al. (2013). IPCC, 2013, *Climate Change 2013—The Physical Science Basis. Climate Change 2013: The Physical Science Basis. Contribution of Working Group I to the Fifth Assessment Report of the Intergovernmental Panel on Climate Change* (pp. 1535). Cambridge, UK: Cambridge University Press. https://doi.org/10.1017/CBO9781107415324

Tebaldi, C., Hayhoe, K., Arblaster, J. M., & Meehl, G. A. (2006). Going to the extremes. *Climatic Change*, *79*(3-4), 185–211. https://doi.org/10.1007/s10584-006-9051-4

Trenberth, K. E., Dai, A., Rasmussen, R. M., & Parsons, D. B. (2003). The changing character of precipitation. *Bulletin of the American Meteorological Society*, *84*(9), 1205–1218. https://doi.org/10.1175/BAMS-84-9-1205

van Oldenborgh, G. J., van der Wiel, K., Sebastian, A., Singh, R., Arrighi, J., Otto, F., et al. (2017). Attribution of extreme rainfall from Hurricane Harvey, August 2017. *Environmental Research Letters*, *12*, 124009. https://doi.org/10.1088/1748-9326/aa9ef2

van der Wiel, K., Kapnick, S. B., van Oldenborgh, G. J., Whan, K., Philip, S., Vecchi, G. A., et al. (2017). Rapid attribution of the August 2016 flood-inducing extreme precipitation in south Louisiana to climate change. *Hydrology and Earth System Sciences*, *21*(2), 897–921. https://doi.org/10.5194/hess-21-897-2017

Vose, R., Easterling, D., Kunkel, K., LeGrande, A., & Wehner, M. (2017). Temperature changes in the United States. In D. J. Wuebbles, et al. (Eds.), *Climate Science Special Report: Fourth National Climate Assessment* (Vol. 1, pp. 185–206). https://doi.org/10.7930/J0N29V45

Wilby, R. L., & Wigley, T. M. L. (2002). Future changes in the distribution of daily precipitation totals across North America. *Geophysical Research Letters*, *29*(7), 1135. https://doi.org/10.1029/2001GL013048

Wilks, D. S. (1995). *Statistical Methods in the Atmospheric Sciences: An Introduction* (467 pp.). Amsterdam, Boston: Academic Press.

Wuebbles, D., Fahey, D., Hibbard, K., Dokken, D., Stewart, B., & Maycok, T. K. (2017). Climate science special report: Fourth National Climate Assessment, Volume I, https://doi.org/10.7930/J0J964J6

Xie, P., Chen, M., Yang, S., Yatagai, A., Hayasaka, T., Fukushima, Y., & Liu, C. (2007). A gauge-based analysis of daily precipitation over East Asia. *Journal of Hydrometeorology*, *8*(3), 607–626. https://doi.org/10.1175/JHM583.1